Time-resolved cyclotron resonance in cuprous oxide

Nobuko Naka,[1,2] Ikuko Akimoto,[3] Masanobu Shirai,[4] and Ken-ichi Kan'no[3]
[1]*Department of Physics, Kyoto University, Kitshirakawa-Oiwake-cho, Sakyo-ku, Kyoto 606-8502, Japan*
[2]*PRESTO, JST, 4-1-8 Honcho Kawaguchi, Saitama 332-0012, Japan*
[3]*Department of Materials Science and Chemistry, Wakayama University, Wakayama 640-8510, Japan*
[4]*Institute for Integrated Cell-Material Sciences, Kyoto University, Yoshida-Ushinomiya-cho, Sakyo-ku, Kyoto 606-8302, Japan*
(Received 4 September 2011; revised manuscript received 27 November 2011; published 19 January 2012)

We have demonstrated cyclotron resonance with a temporal resolution of 15 ns by using an electron-spin-resonance cavity. In an undoped direct-gap semiconductor, cuprous oxide, we observe clear low-field shifts of the cyclotron resonance peaks shortly after generation of photoexcited carriers. Based on the plasma shift of the cyclotron resonance, we evaluate the carrier density and quantitatively discuss the interaction between free carriers and excitons. With increasing time delay, the hole resonance asymptotically reaches the constant value corresponding to an effective mass of 0.575 times the free electron mass, providing a definitive answer to the controversy on the effective mass of holes in cuprous oxide.

DOI: 10.1103/PhysRevB.85.035209 PACS number(s): 76.40.+b, 71.35.Gg

I. INTRODUCTION

Cyclotron resonance (CR) is a standard technique to determine effective masses of carriers in semiconductors. In the past, time-resolved CR was carried out in the microsecond range in indirect-gap semiconductors, such as germanium[1] and silicon,[2] and in doped direct-gap semiconductors, such as gallium arsenide.[3] On the other hand, picosecond time-resolved CR has also been demonstrated by using a free-electron laser system operated at a megahertz repetition rate.[4] However, CR on a nanosecond time scale is unexplored because direct extension of the above schemes is difficult due to the limited pulse width or due to the high repetition rate. In this study, we achieve 15-ns temporal resolution by using a dielectric cavity usually used for electron-spin resonance. In addition to the improvement of the temporal resolution, we evaluate the effect of the changing quality factor of the cavity by measuring both imaginary and real parts of the microwave reflectance.[5] Without distortion of resonance curves as pointed out in Refs. 6 and 7, we analyze the CR spectra, which vary with the time delay after the generation of photoexcited carriers, and quantitatively discuss the interaction of carriers with phonons, excitons, and other carriers.

Our method makes CR measurements applicable to new types of experiments, namely, pursuing dynamics of photoexcited carriers in undoped direct-gap semiconductors. As a prototype of such a system we choose cuprous oxide (Cu_2O), which is known by the long-lived quasiparticle state called the exciton, or an electron-hole pair bound by Coulomb force. The first CR measurement in Cu_2O dates back to that in 1960s using cw photoexcitation sources.[8] Despite the long history, there remains a controversy on the hole effective mass: 0.66 m_0[8–10] versus 0.58 m_0[9,11] depending on the literature, where m_0 is the free-electron mass at rest. Furthermore, recent study by high-resolution spectroscopy reveals that not only orthoexcitons[12] but also the paraexcitons[13] have an effective mass largely different from the sum of electron and hole effective masses. This fact invoked revived interest in the band structure of Cu_2O, leading to a theoretical calculation including the spin-orbit interaction for the full band dispersion.[14] Also, a computational study, which requires the electron and hole effective masses as known parameters, has shown that the central-cell corrections account for the large excitonic mass.[15] Since the excitonic mass is a key parameter determining the critical temperature for a quantum phase transition, such as Bose-Einstein condensation, solving the controversy on the hole effective mass is important.

II. EXPERIMENT

Samples with dimensions of $\sim 3 \times 3 \times 3$ mm^3 were cut from natural crystals mined in Africa. The surface planes were oriented along {001}. An external magnetic field up to 1 T was applied along the [001] crystal axis. A microwave of 0.1 mW at a frequency of $f = 9.68$ GHz irradiated the sample mounted in a quartz tube in the electron-spin-resonance cavity (Bruker, MD5W1) at 10 K in a cryostat. The free carriers are generated under optical excitation by pulsed light from an optical parametric oscillator (Spectra Physics, MOPO) pumped by a Nd:YAG laser. The repetition rate is 10 Hz, the pulse width is 5 ns, and the linewidth is 0.2 cm^{-1}. The pulse energy is 0.8 mJ outside the cryostat. The laser beam is loosely focused on a spot with an area of 3×1.5 mm^2 on the sample surface. Due to the cryostat windows, cavity mesh, and the quartz tubes surrounding the sample, the pulse energy measured by a photodetector (Hamamatsu, S10356-01) at the sample position is a factor of 10 (40) less on the front (side) surface of the sample. The reflected microwave was measured with a bridge (Bruker, ELEXSYS E580). Both of the real and imaginary parts of the microwave signal were recorded with an oscilloscope (SpecJet) as a function of the time delay following the laser pulse. The quality factor of the cavity is set to 800, and the temporal resolution is 15 ns. By analyzing the imaginary parts, we confirm that there is no change in the effective quality factor at times later than 40 ns.[5]

The inset of Fig. 1 shows a schematic diagram of the band structure of Cu_2O near the zone center. The minimum energy gap is called the yellow gap (2.17 eV), and the next one is the green gap (2.30 eV). For most cases (except for Fig. 4), we choose the excitation at the phonon-assisted absorption due to 1s excitons, with which we obtained the strongest microwave absorption. The corresponding photon energy is 2.07 eV, about 0.1 eV below the yellow gap.

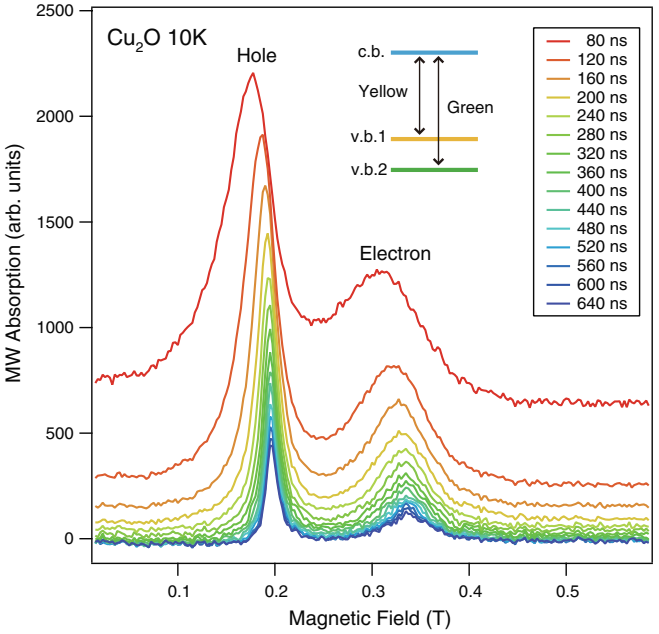

FIG. 1. (Color online) Temporal change of the cyclotron resonance spectrum of Cu_2O at 10 K. The time intervals for adjacent curves are 40 ns, as shown in the legend. The inset shows the band structure of Cu_2O near the zone center. The arrows indicate energy gaps between the conduction band (c.b.) and the valence bands (v.b.1 and v.b.2).

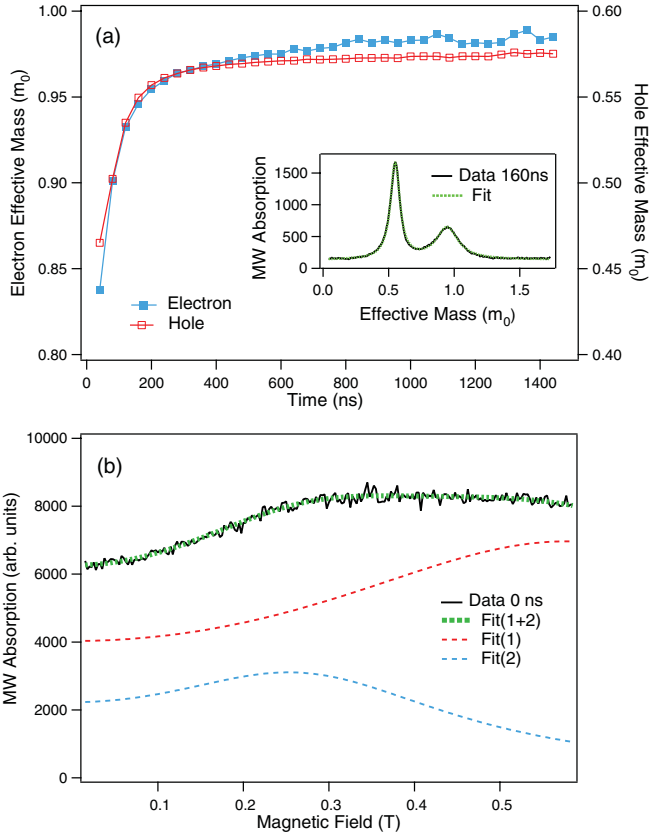

FIG. 2. (Color online) (a) Temporal change of the effective masses for electrons and holes, which are obtained from the resonance magnetic fields. The inset shows the fitting of the cyclotron resonance spectrum to the sum of two Lorentzian functions. The data (solid line) are taken at a delay time of 160 ns. (b) Fitting of the spectrum, centered at $t = 0$ ns and averaged over 20 ns, to the sum of two magnetoplasma resonances.

In our experimental geometry, the densities of the excitons and carriers are inhomogeneous because the absorption length of the incident photons is 0.28 mm (Ref. 16) against the crystal thickness of 3 mm. The spatial inhomogeneity is one limitation of our scheme when a thick sample is used. Based on the measurement of CR signals using a thin (0.3 mm thick) sample located at various positions within the cavity as well as on the measurement of the laser power inside the cavity by the photodetector, we estimate that the major contributions to the microwave absorption come from the front and the side surfaces of the sample. Although the side surface receives only about 20 % of the photons incident on the sample, carriers in the side surface respond with a higher sensitivity compared to those in the middle of the front surface due to the polarization selection rule for the transitions between Landau levels.

III. RESULT AND DISCUSSION

Figure 1 shows a real part of the microwave signal measured at different time delays with a Cu_2O crystal in the electron-spin-resonance cavity at 10 K. The microwave absorption peaks are caused by the cyclotron resonance (CR) of photoexcited carriers. The topmost curve is a spectrum averaged for the delay from $t = 60$ to 100 ns (centered at $t = 80$ ns). Time steps for other curves are 40 ns, as indicated in the legend. Referring to the literature, we assign the low-field peak to holes and the high-field one to electrons. It is clear that each peak changes its position and width depending on the time delay. The peaks show broadening and low-field shifts soon after the photoexcitation. The carriers contributing to the CR signal are produced by ionization of photogenerated excitons, and thus two different kinds of carriers (i.e., electrons and holes) coexist with excitons. In the following considerations, we include line broadening by the interaction between carriers or with excitons as well as the influence of the screening[17] on the peak position and also examine the influence of the coupling between electron plasma and hole plasma.[18]

The inset of Fig. 2(a) shows an example of the fits of a CR spectrum to the sum of two Lorentzian functions. The horizontal axis has been converted to the effective mass using the relation $m^* = eB/\omega$, where B is the magnetic field and $\omega = 2\pi f$ is the angular frequency of the microwave. Almost perfect agreement of the fit to data is obtained. Figure 2(a) is a plot of the effective mass values as a function of time delay. It is found that with increasing delay the hole effective mass monotonically reaches a constant value of $m_h^* = 0.575\ m_0$, which is in agreement with one of the reported values. The electron mass also shows more than $-0.1\ m_0$ shift at early times compared to the value at later times, $m_e^* = 0.985\ m_0$.

For the reason of the mass shifts, one might suspect the heating of the sample by the excess energy shed from the laser. We confirmed that the resonance peak shifts to the high-field side at higher lattice temperatures. The observed shift, however, occurs in the opposite direction. Therefore, we cannot attribute the shifts to a lattice-heating effect. In addition, carrier heating[19] is also unlikely; even when

the free carriers are as hot as 1000 K, the average kinetic energy corresponds to only 0.3% of the Brillouin zone. The nonparabolicity of the valence band is expected around 10% of the Brillouin zone,[14] and the carrier would not gain such a high kinetic energy.

Another possible origin for the shifts is plasma screening. Under the influence of depolarization due to surrounding carriers at a density of $n(t)$ at a time t, the cyclotron resonance frequency changes as[17] $\omega'(t) = \omega - \omega_p(t)^2/\omega$, where $\omega_p(t) = \sqrt{n(t)e^2}/\sqrt{\epsilon_o m^*}$ is the plasma frequency and $\epsilon_o = 6.46$ is the high-frequency dielectric constant of Cu_2O.[20] Since $\omega'(t)$ decreases with increasing carrier density, the peak should show a low-field shift at a higher density. Inversely, the carrier density can be estimated from the peak shift:

$$n(t) = \frac{\epsilon_o \omega}{e}[B_\infty - B(t)], \tag{1}$$

where $B(t)$ is the resonance field at time t and B_∞ is that at late times. This gives a hole density $n_h = (5.42 \pm 0.04) \times 10^{11}$ cm^{-3} and an electron density $n_e = (6.3 \pm 0.2) \times 10^{11}$ cm^{-3} at $t = 80$ ns, for instance. The hole and electron densities at zero time delay should be the same, while the hole density decreases a little faster than the electron density, presumably because of the larger mobility,[21] which causes faster diffusion. The precision of the evaluated densities depends on the width of the CR peaks, and the better precision for the hole density comes from the sharper resonance.

At higher carrier densities where the plasma frequency exceeds the microwave frequency, the carriers exhibit magnetoplasma resonance rather than CR. The threshold density when the plasma frequency equals the microwave frequency is 4.3×10^{12} and 7.4×10^{12} cm^{-3}, respectively for hole and electron plasmas independent from each other. When approaching the threshold density, a coupling can occur between the motions of electron plasma and the hole plasma, leading to further shifts of the peak positions.[18] The difference in the resonance positions, however, assuming coupled or decoupled plasma models for the same carrier density, stays within 8% up to the carrier density (6×10^{11} cm^{-3}) at 80 ns. As the difference becomes smaller with decreasing carrier densities, we neglected the effect of the coupling between hole plasma and the electron plasma for the analysis of the data taken at a time later than 80 ns.

Because the threshold densities in the decoupled plasma model are only several times the estimated densities at $t = 80$ ns, magnetoplasma resonance is expected to occur for earlier times. In Fig. 2(b), the microwave absorption measured at $t = 0$ is shown by the black line. A broad feature without CR peaks is seen. We fit this spectrum with the sum of magnetoplasma resonances:[17]

$$M(B) = \Sigma_i \frac{A_i\left(\Gamma_i^2 + B_i^2 + B^2\right)}{1/\Gamma_i^2\left(\Gamma_i^2 - B_i^2 + B^2\right)^2 + 4B_i^2}. \tag{2}$$

We assume two components ($i = 1,2$) by taking into account the contributions from the front and side surfaces. The fitting function is shown by the green dotted line. The parameters chosen are $B_1 = -0.59$ T and $\Gamma_1 = 0.41$ T for the first component, shown by the red line, and $B_2 = -0.27$ T and $\Gamma_2 = 0.22$ T for the second component, shown by the blue line. Comparison of Figs. 1 and 2 tells us that carriers exhibit a transient shift with increasing time delay from magnetoplasma resonance into plasma-shifted CR. In Fig. 1, in addition to the CR peaks a background component appears more significantly at early times. We attribute this background component to the magnetoplasma resonance of carriers near the front surface. The CR peaks are attributed to carriers near the side surface,

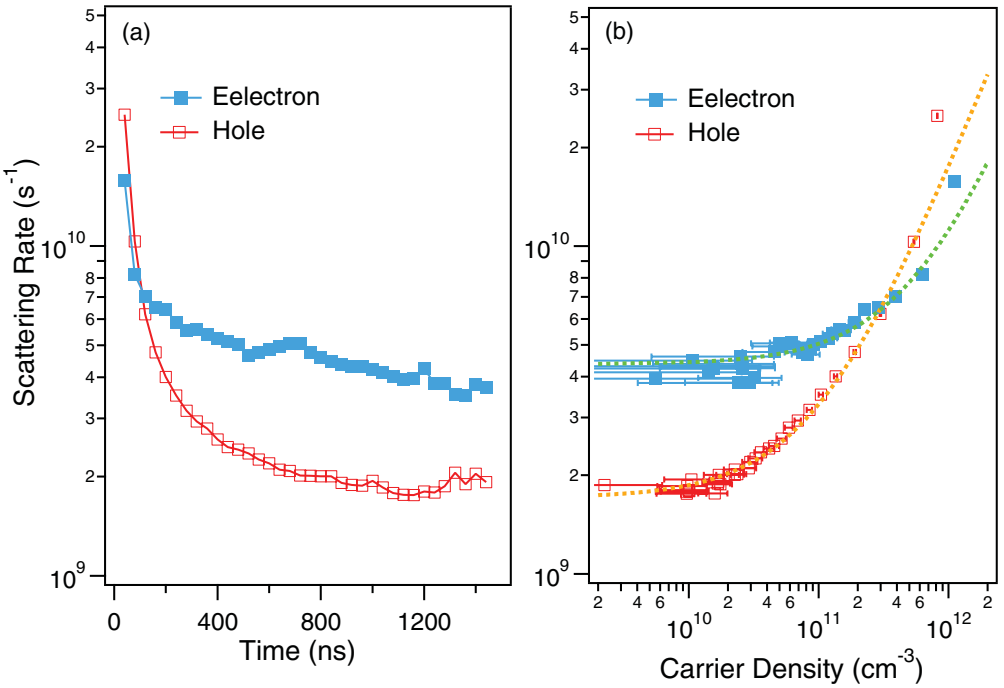

FIG. 3. (Color online) (a) Scattering rates for electrons and holes, obtained from the linewidth of the cyclotron resonance peaks, as a function of time delay. (b) Scattering rates as a function of the carrier density estimated from the plasma shift of the CR peaks.

since CR occurs at a lower density than for the magnetoplasma resonance.

Aside from the carrier densities, the CR spectra shown in Fig. 1 provide information on the scattering rate, $1/\tau$, of carriers. The scattering rate is obtained by $1/\tau = \omega\Delta B/B$, with the resonance field B and the half width ΔB. Figure 3(a) is a plot of the scattering rate as a function of time delay. The scattering rate decreases with time and mostly is in the range of 10^9 s^{-1}. Figure 3(b) is a plot of the scattering rate versus carrier density n, estimated by using Eq. (1). It is found that the scattering rate changes linearly to the carrier density. The dotted curves are fits to a linear function with an offset: $1/\tau = c + bn$. For the best fit we obtained $c_h = (1.7 \pm 0.1) \times 10^9$ s^{-1} and $c_e = (4.1 \pm 0.2) \times 10^9$ s^{-1}, $b_h = 0.0159 \pm 0.0002$ cm^3 s^{-1} and $b_e = 0.0068 \pm 0.0004$ cm^3 s^{-1}, where subscripts h and e denote holes and electrons, respectively.

First, we discuss the origin of the offsets, c_h and c_e, namely, the scattering rates at the low-density limit. The longitudinal acoustic phonon scattering of carriers at momentum k occurs with a rate[22]

$$1/\tau_{\mathrm{LA}}(k) = \frac{D^2 m^*}{4\pi\hbar^2 k\rho v_l}\left[\int_{L_1}^{L_2}\frac{q^2dq}{e^{\hbar v_l q/k_BT}-1} + \int_0^{L_3}\frac{q^2dq}{1-e^{-\hbar v_l q/k_BT}}\right], \quad (3)$$

where $\rho = 6.1$ g/cm^3 is the density of Cu_2O, $v_l = 4.63 \times 10^3$ m/s is the velocity of the LA phonon, and D is the deformation potential. The integration limits are[22] $L_1 = 2(m^* v_l/\hbar - k)$ or 0, $L_2 = 2(m^* v_l/\hbar + k)$, and $L_3 = 0$ or $2(k - m^* v_l/\hbar)$ for $k < m^* v_l/\hbar$ or $k \geqslant m^* v_l/\hbar$. We approximate the deformation potentials for holes and electrons by that for excitons ($D = 1.68$ eV) and take thermal average over k. We obtain $1/\tau_{\mathrm{LA}} = 1.56 \times 10^9$ and 3.30×10^9 s^{-1} for holes and electrons at 10 K, respectively.[23] The estimated c_h and c_e are close to these values, implying that the scattering at low carrier densities is dominated by acoustic-phonon scattering.

Next, we consider the second term. The linear dependence to the carrier density n implies that the scattering is governed by the interaction with excitons whose density changes proportionally to n or by that with carriers at high temperatures where Coulomb repulsion is insignificant. The boundary temperature for the Coulomb repulsion is obtained as $T_b = 86$ K for Cu_2O by equating the phase shift $e^2 m^{*1/2}\omega_c (k_BT)^{-3/2}/\epsilon_o$ to unity.[3] Since the lattice temperature is well below T_b, the carrier-carrier scattering should occur proportionally to $n^{1/2}$ instead of n. On the other hand, a carrier-exciton interaction predicts a scattering rate changing linearly to the exciton density N_{ex}.

Here we note that the cyclotron radii, $l_h = \sqrt{\hbar/(\omega m_h^*)} = 58$ nm and $l_e = \sqrt{\hbar/(\omega m_e^*)} = 44$ nm, are much larger than the excitonic Bohr radius and even larger than the de Broglie length. Therefore, we treat the carrier-exciton interaction as a classical collision by assuming the scattering rate to be

$$1/\tau_{e(h)-\mathrm{ex}} = N_{\mathrm{ex}} v_{e(h)} \sigma_{e(h)}, \quad (4)$$

where $v_{e(h)} = \sqrt{3k_BT/m_{e(h)}^*}$ is the thermal velocity of the carriers. We take the scattering cross section, $\sigma_e \sim 43\pi a_B^2$, according to numerical calculation for electrons in Cu_2O by Elkomoss *et al.*[24] For the incident photons at 2.07 eV, 100% conversion efficiency from photons to excitons has been measured.[16] Therefore, the incident pulse of 0.8 mJ outside the cryostat corresponds to an exciton density of $N_{\mathrm{ex}}(0) = 18.9\ (4.73) \times 10^{16}$ cm^{-3} at the front (side) sample surface. This density is high enough to cause two-body collisions accompanied by the formation of free carriers. We expect that the exciton density is decreased with increasing time delay and that no further ionization of excitons into free carriers occurs at times later than 80 ns. In fact, the temporal change of the carrier density presently observed is not far from that of the exciton density we reported before.[25] Then the scattering rate changes almost linearly to the carrier density via Eq. (4). In order to match $1/\tau_{e-\mathrm{ex}} (= N_{\mathrm{ex}} v_e \sigma_e)$ with $b_e n_e$, we get $N_{\mathrm{ex}}(t) = 6.5 \times 10^3 n_e(t)$. Using the electron density contributing to the CR, $n_e = 6.3 \times 10^{11}$ cm^{-3}, at $t = 80$ ns, the exciton density at $t = 80$ ns is calculated as $N_{\mathrm{ex}} = 3.9 \times 10^{15}$ cm^{-3}. This is reasonable considering the decrease of the exciton density by one order of magnitude within 80 ns.

We emphasize that we generate excitons at the phonon-assisted absorption edge below the yellow gap so that there should be no free carriers directly generated. Nevertheless, the observed CR signal implies the existence of free carriers. In order to confirm that the free carriers arise from excitons, we studied the dependence of the CR signal on the photon energy of incident light. For comparison, absorption spectra of Cu_2O at 2 K are shown in Fig. 4(a). The absorption starts as the square-root function of energy from the phonon-assisted absorption edge of 1s excitons. Yellow and green excitonic

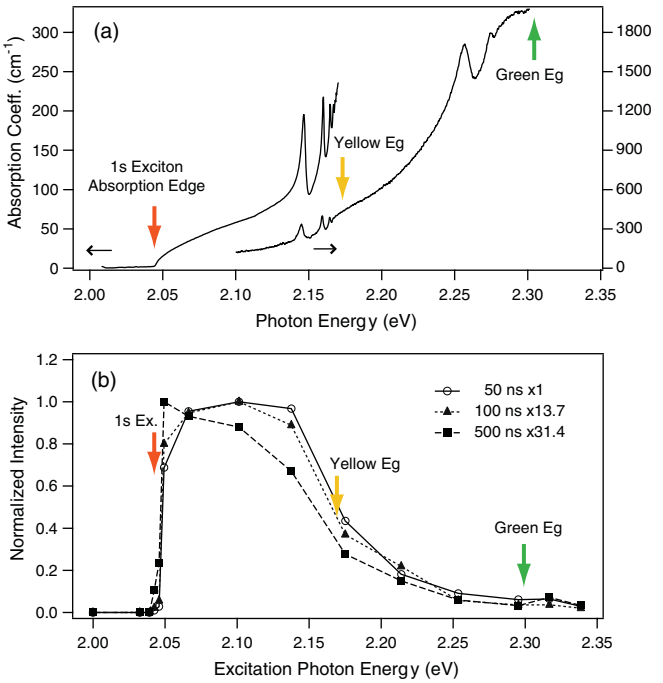

FIG. 4. (Color online) (a) Absorption spectra at 2 K, displayed in different vertical scales. The energy positions of the absorption edge of 1s excitons, the yellow gap, and the green gap are indicated by vertical arrows. (b) Intensity of the cyclotron resonance peak for holes as a function of incident photon energy. Microwave absorption intensities at three different times are plotted after normalization.

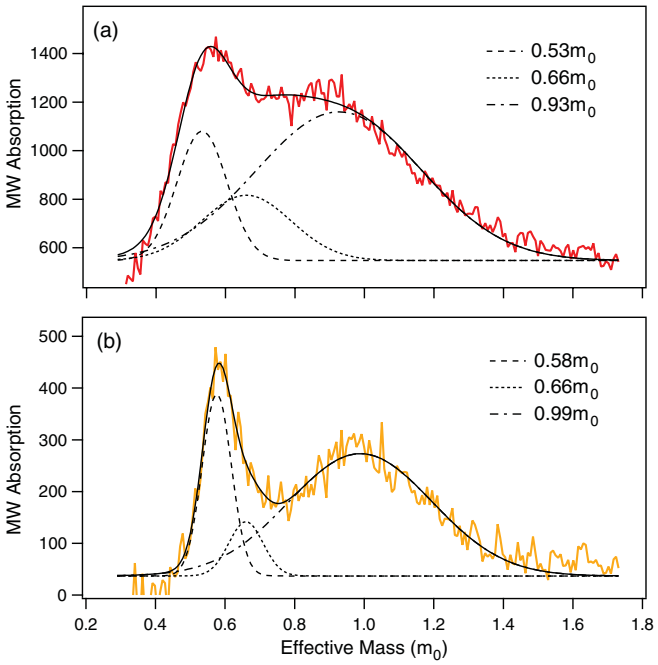

FIG. 5. (Color online) Cyclotron resonance spectra obtained with a vacancy-rich sample at a time delay of (a) 50 ns and (b) 170 ns. The black lines show fitting results with the sum of three Gaussian functions.

series are seen below the yellow and green gaps indicated by vertical arrows. Figure 4(b) shows the intensity of the CR peak for holes as a function of the incident photon energy. For this plot, we first fit the CR spectrum with a sum of two Lorentzian functions plus a background component and then calculated the areal intensity of the hole peak using the fitting function to reduce the noise. The data points are normalized at the maximum intensity at respective time delays, with the normalization factor indicated in the legend in Fig. 4(b). Vertical arrows indicate the positions of the absorption edge of 1*s* excitons, the yellow gap, and the green gap at 10 K, which are shifted by 4 meV compared to those in Fig. 4(a) to include the temperature shift of the energy gap. Interestingly, the CR signal does not appear with photon energies below 2.04 eV and shows an abrupt increase for larger photon energies. The photon energy for the abrupt increase exactly agrees with that for the phonon-assisted absorption edge of the 1*s* excitons, indicating that the CR signal comes via generation of 1*s* excitons. The signal gradually decreases with increasing photon energy, particularly above the yellow gap. This is probably due to less spatial overlap between the microwave and carrier distributions.[5] Above the green gap, the signal is very weak but takes finite values. We found that the photon-energy dependence exhibits a gradual change with increasing time delay. The change is most pronounced around the absorption edge, where a sharper rise is seen at later times. This means that the free carriers generated from the excitons with smaller kinetic energy live a longer life.

Finally, we comment on the hole mass of 0.66 m_0 reported in some studies.[8–10] Using a sample cut from a different mother crystal containing more vacancies, we observed a signal around 0.66 m_0, overlapping to the peak centered at 0.58 m_0, as shown in Fig. 5. The solid lines represent the fitting results from the sum of three Gaussian functions. The fact that CR spectra fit well with the sum of three Gaussian functions rather than a sum of two Lorentzian functions implies some extrinsic effect. Each component of the Gaussian functions is shown by dotted, dashed, and dash-dotted lines. We find that the peak at 0.66 m_0 decays faster than the peak at 0.58 m_0, while the widths of these peaks are similar. Based on these facts, we conclude that the effective mass of 0.66 m_0 is not from the bottom of the highest valence band. This might be due to band warping or the second valence band located deeper in energy.

IV. CONCLUSION

We have established the method of measuring cyclotron resonance using an electron-spin-resonance cavity with nanosecond temporal resolution under photoexcitation of an undoped semiconductor. Interactions of excitons with acoustic phonons or with free carriers were investigated based on the scattering rates obtained for different carrier densities at different time delays. This method is ready to be applied to other materials having a relaxation time in a range between nanoseconds and microseconds, which had been difficult to access with conventional cyclotron resonance methods.

ACKNOWLEDGMENTS

This work was partially supported by the Grant-in-Aid for Young Scientists (B) (Grant No. 21740227) of JSPS, Japan, the Grant-in-Aid for Scientific Research on Innovative Areas "DYCE" (Grants No. 20104002 and No. 23104720) of MEXT, Japan, and by the Asahi Glass Foundation.

[1]T. Ohyama, T. Sanada, T. Yoshihara, K. Murase, and E. Otsuka, Phys. Rev. Lett. **27**, 33 (1971).
[2]T. Ohyama, T. Sanada, and E. Otsuka, J. Phys. Soc. Jpn. **35**, 822 (1973).
[3]T. Ohyama, J. Phys. Soc. Jpn. **51**, 1431 (1982).
[4]G. A. Khodaparast, D. C. Larrabee, J. Kono, D. S. King, S. J. Chung, and M. B. Santos, Phys. Rev. B **67**, 035307 (2003).
[5]I. Akimoto, N. Naka, M. Shirai, and K. Kann'no (unpublished).
[6]H. E. Porteanu, Rev. Sci. Instrum. **76**, 035106 (2005).
[7]S. Grabtchak and M. Cocivera, Phys. Rev. B **58**, 4701 (1998).
[8]A. I. Gubanov, N. I. Krivko, and N. M. Reinov, Zh. Eksp. Teor. Fiz. **38**, 341 (1960) [Sov. Phys. JETP **11**, 247 (1960)].
[9]J. W. Hodby, T. E. Jenkins, C. Schwab, H. Tamura, and D. Trivich, J. Phys. C **9**, 1429 (1976).
[10]A. Golzene and C. Schwab, Solid State Commun. **18**, 1565 (1976).
[11]T. Ohyama, T. Ogawa, and H. Nakata, Phys. Rev. B **56**, 3871 (1997).

[12]N. Caswell, J. S. Weiner, and P. Y. Yu, Solid State Commun. **40**, 843 (1981).
[13]J. Brandt, D. Fröhlich, C. Sandfort, M. Bayer, H. Stolz, and N. Naka, Phys. Rev. Lett. **99**, 217403 (2007).
[14]M. French, R. Schwartz, H. Stolz, and R. Redmer, J. Phys. Condens. Matter **21**, 015502 (2008).
[15]A. Alvermann, P. B. Littlewood, and H. Fehske, Phys. Rev. B **84**, 035126 (2011).
[16]K. E. O'Hara, J. R. Gullingsrud, and J. P. Wolfe, Phys. Rev. B **60**, 10872 (1999).
[17]G. Dresselhaus, A. F. Kip, and C. Kittel, Phys. Rev. **100**, 618 (1955).
[18]R. E. Michel and B. Rosenblum, Phys. Rev. Lett. **7**, 234 (1961); Phys. Rev. **128**, 1646 (1962).
[19]J. C. Hensel and G. Feher, Phys. Rev. **129**, 1041 (1963).
[20]M. O'Keeffe, J. Chem. Phys. **39**, 1789 (1963).
[21]T. Ito, H. Yamaguchi, K. Okabe, and T. Masumi, J. Mater. Sci. **33**, 3555 (1998).
[22]D. P. Trauernicht and J. P. Wolfe, Phys. Rev. B **33**, 8506 (1986).
[23]These values are slightly smaller than the values obtained from Eq. (4) in Ref. 11. The correction comes from the fact that fewer channels exist for scattering at lower temperatures due to energy and momentum conservations.
[24]S. G. Elkomoss and G. Munschy, J. Phys. Chem. Solids **38**, 557 (1977).
[25]N. Naka and N. Nagasawa, Phys. Rev. B **65**, 075209 (2002).